Spinophilin regulates the formation and function of dendritic spines

Jian Feng*†, Zhen Yan*, Adriana Ferreira‡, Kazuhito Tomizawa*, Jason A. Liauw§, Min Zhuo§, Patrick B. Allen*, Charles C. Ouimet¶, and Paul Greengard*

*Laboratory of Molecular and Cellular Neuroscience, The Rockefeller University, New York, NY 10021; ‡Department of Cell and Molecular Biology, Northwestern Institute for Neuroscience, Northwestern University, Chicago, IL 60611; §Department of Anesthesiology, Department of Anatomy and Neurobiology, Washington University, St. Louis, MO 63110; and ¶Program in Neuroscience, Florida State University, Tallahassee, FL 32306

Contributed by Paul Greengard, May 30, 2000

Spinophilin, a protein that interacts with actin and protein phosphatase-1, is highly enriched in dendritic spines. Here, through the use of spinophilin knockout mice, we provide evidence that spinophilin modulates both glutamatergic synaptic transmission and dendritic morphology. The ability of protein phosphatase-1 to regulate the activity of α-amino-3-hydroxy-5-methyl-4-isoxazolepropionic acid (AMPA) and *N*-methyl-D-aspartate (NMDA) receptors was reduced in spinophilin knockout mice. Consistent with altered glutamatergic transmission, spinophilin-deficient mice showed reduced long-term depression and exhibited resistance to kainate-induced seizures and neuronal apoptosis. In addition, deletion of the spinophilin gene caused a marked increase in spine density during development *in vivo* as well as altered filopodial formation in cultured neurons. In conclusion, spinophilin appears to be required for the regulation of the properties of dendritic spines.

Dendritic spines are specialized protrusions from dendritic shafts that receive the vast majority of excitatory input in the central nervous system (1). Dynamic changes in the number, size, and shape of dendritic spines have been associated with learning (2, 3), electrophysiological (4–6), developmental (7, 8), and hormonal changes (9, 10). It is increasingly evident that alterations in synaptic activity can cause morphological changes of dendritic spines (2, 11–14): high-intensity stimulation of CA1 neurons induces rapid formation of spine-like protrusions (or filopodia) (12), and decreased synaptic activity results in loss of dendritic spines (14). Conversely, morphological changes in dendritic spines have profound effects on their electrical and biochemical properties (15–17), thereby regulating the efficacy of synaptic transmission (13, 18, 19). However, with the exception of evidence that localization of glutamate receptors is altered with neuronal activity (20, 21), little is known about the molecular mechanisms underlying the linkage between synaptic activity and the dynamic morphological changes of dendritic spines.

Spinophilin, also called neurabin II (22), interacts with several proteins that are highly enriched in spines (22, 23). One of them, actin, is important for the formation, maintenance, and morphology of spines (18). *In vitro*, spinophilin bundles actin filaments (22), suggesting its possible role as one organizer of the actin-based cytoskeleton in dendritic spines. Another binding partner of spinophilin that is enriched in dendritic spines is protein phosphatase-1 (PP-1) (23, 24). There is evidence that PP-1 modulates the activity of a variety of ion channels, including glutamate receptors (25–28). These properties of spinophilin make it an attractive candidate for regulating the dynamic morphological and functional changes that occur in dendritic spines. To investigate the possible role of spinophilin in spine formation and function, we used gene-targeting methods to generate mice that lack the expression of spinophilin.

Methods

Generation of Spinophilin Knockout Mice. The targeting vector consisted of a 3.5-kb left arm and a 4.0-kb right arm, derived from genomic DNA flanking the first exon of spinophilin. A 1.1-kb neo^R cassette was put in reverse orientation to replace the 4.2-kb *Bam*HI fragment containing exon 1. The construct was electroporated into RW4 cells (Genome Systems, St. Louis), following the manufacturer's procedures. Positive clones (4/192) were identified by PCR and Southern blot and were injected into C57BL/6 blastocysts. Three highly chimeric males were derived and bred with C57BL/6 females to obtain germ-line transmission. The resulting spinophilin$^{+/-}$ mice were intercrossed to produce three lines of spinophilin$^{-/-}$ mice. Southern blots were carried out on *Eco*RV digests of tail DNA with [^{32}P]dCTP-labeled external probe. Animal use and care were in strict accordance with protocols approved by the Institutional Animal Care and Use Committees at the investigators' universities.

Biochemical Measurements. Whole brains from wild-type and knockout littermates ($n = 6$ for each group) were homogenized in 10 ml of 1% SDS solution. Protein concentration of brain homogenates was measured with the DC Protein Assay Kit (Bio-Rad). To measure the expression level of various proteins, an equal amount (100 μg) of total brain protein from animals of different genotypes was run on SDS/PAGE gel and Western blots were performed with the following antibodies. Spinophilin antibodies were made against two peptides corresponding to amino acids 367–390 (23) and 790–808. Neurabin antibody was raised against the peptide from amino acids 885–903. Antibodies against GluR1 and NR1 were purchased from Upstate Biotechnology. All data in this paper are expressed as means ± SEM. Student's *t* tests were performed to assess statistical significance.

Neuroanatomical Measurements. Thickness of hippocampal layers from adult mice was measured on cresyl violet-stained brain sections ($n = 4$ mice for each genotype). Volume of the hippocampus was measured by the Cavalieri method (29) in the brains of mice 10–14 weeks old. Serial sections (100 μm thick) were taken in the coronal plane from four knockout and four wild-type brains. The identity of the brains was coded while the measurements were taken. Starting with the first or second section (randomly chosen), the area of the hippocampus was measured on every third section. The mean area from all of the measured sections then was multiplied by section thickness times the total number of sections to estimate hippocampal volume.

Abbreviations: LTP, long-term potentiation; LTD, long-term depression; NMDA, *N*-methyl-D-aspartate; AMPA, α-amino-3-hydroxy-5-methyl-4-isoxazolepropionic acid; PP-1, protein phosphatase-1; TUNEL, terminal deoxynucleotidyltransferase-mediated dUTP end labeling; P15, postnatal day 15; PTZ, pentylenetetrazole.

†To whom reprint requests should be addressed at: Laboratory of Molecular and Cellular Neuroscience, The Rockefeller University, 1230 York Avenue, New York, NY 10021. E-mail: fengji@rockvax.rockefeller.edu.

The publication costs of this article were defrayed in part by page charge payment. This article must therefore be hereby marked "*advertisement*" in accordance with 18 U.S.C. §1734 solely to indicate this fact.

Histological Procedures. Mice were perfused transcardially with 4% formaldehyde in PBS. After 1 h of postfixation *in situ*, brains were removed and stored overnight in fixative at 4°C. Vibratome sections (100 μm) were stained with a single-section Golgi technique (30). In brief, sections were incubated in osmium tetroxide (1% in PBS) for 30 min, rinsed in PBS (three times for 10 min each), incubated in potassium dichromate (3.5% aqueous) for 1.5 h, and mounted between two microscope slides. The slides were fastened together at the top with electrical tape and immersed in silver nitrate (1% aqueous) overnight. An insufficient number of neurons was impregnated in the hippocampus, and we therefore examined dendritic spine density in the caudatoputamen. Secondary dendrites were drawn with a camera lucida, and the number of spines per unit length of dendrite was counted. A group of four knockouts and four wild-type littermates was analyzed at postnatal day 15 (P15), and a second group of four knockouts and four wild-type littermates was analyzed at 2–3 months. Spines were counted on 58 segments of secondary dendrites (total dendritic length of 4,152 μm) for P15 mice and 54 segments of secondary dendrites (total dendritic length of 4,225 μm) for adult mice. In total, more than 8,000 spines were counted.

Hippocampal Cultures and Immunocytochemistry. Neuronal cultures were prepared from the hippocampi of wild-type and spinophilin knockout embryos at embryonic day 16 as described previously (31). Cultures at 7, 14, and 21 days *in vitro* were fixed for 20 min with 4% paraformaldehyde in PBS containing 0.12 M sucrose and then permeabilized in 0.3% Triton X-100 in PBS for 5 min and rinsed twice in PBS. The cells were preincubated in 10% BSA in PBS for 1 h at 37°C, exposed to primary antibodies (diluted in 1% BSA in PBS) overnight at 4°C, and then rinsed in PBS and incubated with secondary antibodies for 1 h at 37°C. The following antibodies were used: mouse anti-tubulin (clone DM1A) (Sigma), rabbit anti-synaptophysin (Roche Molecular Biochemicals, Indianapolis, IN), fluorescein-conjugated anti-mouse IgG, and rhodamine-conjugated anti-rabbit IgG (Roche). Rhodamine-conjugated phalloidin was used to stain actin filaments.

Electrophysiology. Whole-cell patch–clamp recording was performed on acutely dissociated striatal and hippocampal neurons from 3- to 4-week-old wild-type and knockout littermates as described previously (26). Kainate (200 μM) was applied briefly (2–4 sec) every 30 sec to evoke α-amino-3-hydroxy-5-methyl-4-isoxazolepropionic acid (AMPA) receptor currents. *N*-methyl-D-aspartate (NMDA; 100 μM) was applied in the same manner to evoke NMDA receptor currents in Mg^{2+}-free solution. Data were collected with PCLAMP software and analyzed with AXOGRAPH, KALEIDOGRAPH, and STATVIEW. Long-term depression (LTD) and long-term potentiation (LTP) studies were carried out in 4- to 6-week-old wild-type and knockout littermates as described previously (32). A bipolar tungsten stimulating electrode was placed in the stratum radiatum in the CA1 region, and extracellular field potentials were recorded by using a glass microelectrode (3–12 MΩ, filled with artificial cerebrospinal fluid) also in the stratum radiatum. Stimulus intensity was adjusted to produce a response of approximately 1 mV amplitude, with an initial slope of approximately -0.5 mV/msec. Test responses were elicited at 0.02 Hz. Homosynaptic LTD was induced by prolonged low-frequency stimulation (1 Hz for 15 min). LTP was induced by tetanic stimulation (100 Hz twice for 1 sec with a 20-sec interval). Paired-pulse facilitation of the response at various interpulse intervals (25–400 msec) also was measured. Experiments were performed blind to genotype.

Convulsant-Induced Seizures and Neuronal Apoptosis. Spinophilin knockout mice and wild-type littermates were injected with kainate (Research Biochemicals) or pentylenetetrazole (PTZ; Sigma) i.p. Seizures were scored over a 2-h period according to an arbitrary scale (33): 0, no seizure; 1, 1 seizure; 2, 2–5 seizures; 3, 6–10 seizures; 4, >10 seizures; 5, death or continuous tonic clonic seizures. A partial seizure was counted as half a seizure. One week after injection of kainate, mice were fixed by transcardial perfusion with 4% paraformaldehyde. The brains were coronally sectioned into 28-μm-thick slices by using a cryostat. The sections were stained with 0.1% cresyl violet, and terminal deoxynucleotidyltransferase-mediated dUTP end labeling (TUNEL) assay was performed by using the *in situ* cell death detection kit (Roche) according to the manufacturer's procedures. TUNEL staining was observed by both light and confocal microscopy.

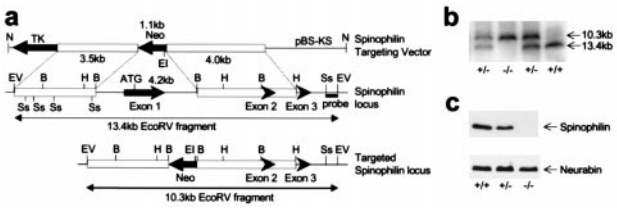

Fig. 1. Generation of spinophilin knockout mice. (*a Top*) Spinophilin targeting vector consisted of a 3.5- and 4.0-kb homologous region flanking the neo^R gene to replace the 4.2-kb *Bam*HI fragment containing exon 1. (*Middle*) Structure of the spinophilin locus showing the first three exons. (*Bottom*) Structure of the targeted spinophilin locus. External probe used for Southern blots is shown. Restriction enzyme sites are indicated: EV, *Eco*RV; Ss, *Sst*I; B, *Bam*HI; H, *Hin*dIII; EI, *Eco*RI; N, *Not*I. (*b*) Southern blot of *Eco*RV-digested tail DNA from wild-type (+/+), heterozygous (+/−), and homozygous (−/−) littermates. (*c*) Western blot analysis of expression levels of spinophilin and neurabin in brain homogenates from wild-type, heterozygous, and homozygous littermates.

Results

Generation of Spinophilin Knockout Mice. Standard gene-targeting methods were used to generate mice that did not express spinophilin. A targeting vector was constructed to replace a 4.2-kb fragment containing the first exon of spinophilin with a neomycin-resistance selection marker. After homologous recombination in embryonic stem (ES) cells, the targeted allele contained a 10.3-kb *Eco*RV fragment, whereas the wild-type allele had a 13.4-kb *Eco*RV fragment (Fig. 1*a*). Four positive ES cell clones were obtained, and three of them produced germ-line transmission of the targeted allele. Southern blot analysis of tail DNA from F1 littermates of intercrosses between heterozygotes demonstrated the disruption of the spinophilin gene (Fig. 1*b*). The absence of spinophilin protein in the knockouts was shown by Western blots of total brain homogenates with two independent antibodies, one raised against the C terminus (Fig. 1*c*) and one against a middle region (23) of spinophilin (data not shown). The expression level of spinophilin in the heterozygous mice was reduced slightly compared with the wild-type mice. No change was observed in the expression level of the spinophilin homologue, neurabin (34), also called neurabin I (22) (Fig. 1*c*). Mendelian distribution of the knockout mice showed that no lethality resulted from disruption of the spinophilin gene. The three independently derived lines of knockout mice exhibited virtually identical phenotypes.

Reduced Brain Size in Spinophilin Knockout Mice. There was a small reduction in body weight in the spinophilin knockout mice [wild type: 31.1 $\pm$ 1.2 g, $n = 11$; knockout: 26.9 $\pm$ 1.6 g, $n = 11$; $P < 0.01$]. The total amount of protein in brains from the knockouts was decreased to 77.8 $\pm$ 1.9% of that in the wild-type mice ($n = 6$, $P < 0.001$), as revealed by protein concentration assays on

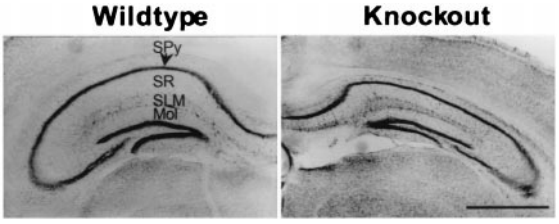

Fig. 2. Reduced size of hippocampus in spinophilin knockout mice. Cresyl violet staining of coronal sections of brain from wild-type and knockout mice. SPy, stratum pyramidale; SR, stratum radiatum; SLM, stratum lacunosum moleculare; Mol, dentate gyrus molecular layer. (Bar = 1 mm.)

whole brains homogenized in 1% SDS. Consistent with this observation, the brain size of the knockouts was also smaller than that of the wild type. This was particularly apparent in the hippocampus, where spinophilin is most highly expressed (23) (Fig. 2). Morphometric measurements showed that there was a significant decrease in the thickness of several hippocampal layers: stratum pyramidale was reduced by 38.4 ± 3.7% ($n = 4$, $P < 0.001$), stratum radiatum was reduced by 33.9 ± 2.0% ($n = 4$, $P < 0.05$), stratum lacunosum moleculare was reduced by 19.5 ± 1.8% ($n = 4$, $P < 0.05$), and dentate gyrus molecular layer was reduced by 19.5 ± 3.4% ($n = 4$, $P < 0.05$). Consequently, when we measured the volume of hippocampi from spinophilin knockout mice and wild-type littermates by using the Cavalieri estimator on serial sections, the size of the hippocampus in spinophilin knockout was reduced by 38.9 ± 5.2% ($n = 4$, $P < 0.01$). Although the basis for this decrease is not clear, the interaction between spinophilin and p70 S6 kinase ($p70^{S6k}$) (P.B.A. and P.G., unpublished observation) might provide an explanation, because $p70^{S6k}$ is a key enzyme in the regulation of protein synthesis (35, 36).

Increased Number of Dendritic Spines in Young Spinophilin Knockout Mice. Because spinophilin is a cytoskeletal protein that is highly enriched in dendritic spines (23), we examined its possible role in spine formation. Golgi staining was performed to study the morphological details of spinophilin-deficient neurons. We counted spines in caudatoputamen from spinophilin knockout and wild-type littermates ($n = 4$ for each group). This analysis revealed more spines per unit length of dendrite in neurons from young knockout mice (Fig. 3). At P15, there were 8.1 ± 0.3 spines per 10 μm of secondary dendrites in wild-type neurons. In comparison, spine density in spinophilin-deficient neurons was 10.9 ± 0.8/10 μm dendrite (Fig. 3*c*). Although spine density was significantly higher in the knockout (34.6 ± 4.7% increase, $P = 0.01$ vs. wild type), the size, shape, and variability of spines did not seem to be significantly different from that of the wild-type littermates. The increase in spine density became statistically insignificant in adult animals [wild type (WT): 10.0 ± 0.5/10 μm; knockout (KO): 11.0 ± 0.6/10 μm, $P > 0.5$ vs. WT; Fig. 3*c*].

To further characterize dendritic morphology in the knockout mice, we cultured hippocampal neurons at low density to estimate the number of spine-like protrusions (or filopodia) and synapses. Cells were stained at various intervals with the F-actin stain, phalloidin, or anti-tubulin to determine the number of spine-like protrusions or with anti-synaptophysin to determine the number of synaptic terminals. In contrast to high-density cultures (37), in our low-density cultures, filopodia appeared somewhere between 14 and 21 days *in vitro*. In cultures from the knockout mice, these filopodia were present much earlier in development and in much larger numbers (Table 1). However, the number of synaptophysin puncta was similar in the knockout and wild-type cultures at each time point (Table 1).

During normal development, spinophilin presumably facilitates the retraction of filopodia or suppresses their initial outgrowth from the dendrite. The lack of significant increase in spine density in the knockout mice at adult age could be due to compensatory responses that prune the extra filopodia formed during development.

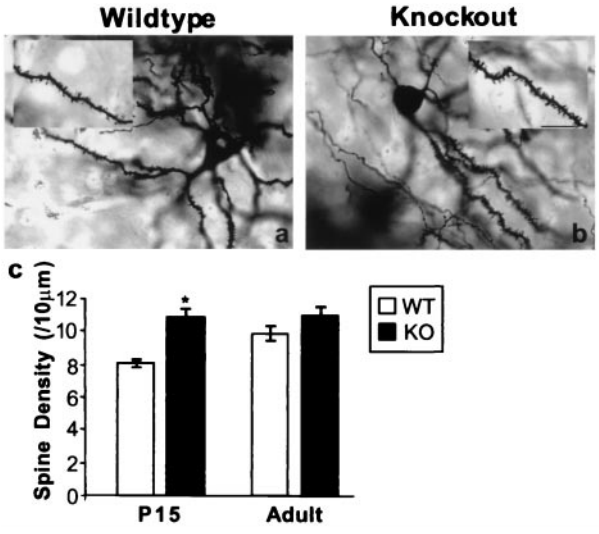

Fig. 3. Increased number of dendritic spines in young spinophilin knockout mice. (*a* and *b*) Representative Golgi staining of a neuron in caudatoputamen from wild-type (*a*) and knockout (*b*) littermates. (Bar = 100 μm.) (*c*) Spine density in wild-type (WT) and knockout (KO) littermates at P15 and adulthood. *, $P = 0.01$, compared with WT at P15.

Regulation of AMPA and NMDA Receptors Is Altered in Spinophilin Knockout Mice. Because AMPA and NMDA receptors are highly enriched in dendritic spines, we compared glutamate receptor currents in wild-type and spinophilin knockout mice. No change was observed in the expression level of the AMPA receptor GluR1 subunit or the NMDA receptor NR1 subunit (data not shown). Using whole-cell patch–clamp recording of acutely dissociated striatal neurons, which retain proximal processes but do not have synapses, we found that the PP-1-mediated "run-down" of AMPA receptor currents (26) seen in the wild-type mice was greatly reduced in the knockouts. In the wild-type neurons, the amplitude of AMPA receptor currents gradually declined over 10 min of recording to 74.5 ± 2.7% of the initial value ($n = 8$). In contrast, in neurons from the knockout mice, the current at 10 min was 94.1 ± 2.2% of the initial value ($n = 8$, $P < 0.01$ vs. wild type). A representative experiment is shown in Fig. 4 *a* and *b*. These data are consistent with a role for spinophilin in the targeting of PP-1 to AMPA receptors, thereby promoting its down-regulation (26).

Table 1. Number of spine-like protrusions and synaptophysin puncta in hippocampal cultures

	Spine-like protrusions/100 μm		Synaptophysin puncta/100 μm	
Days *in vitro*	Wild type	Knockout	Wild type	Knockout
7	0	38 ± 5*	9 ± 0.5	10 ± 0.5
14	0	43 ± 8*	8 ± 0.4	9 ± 0.7
21	13 ± 2	46 ± 4*	10 ± 0.9	9 ± 0.8

Neurons were stained with antibodies against tubulin (to count spine-like protrusions) and synaptophysin (to count synaptophysin puncta). Sixty neurons from three cultures were analyzed for each time point. Results are expressed as means ± SEM. *, $P < 0.001$, compared with wild type.

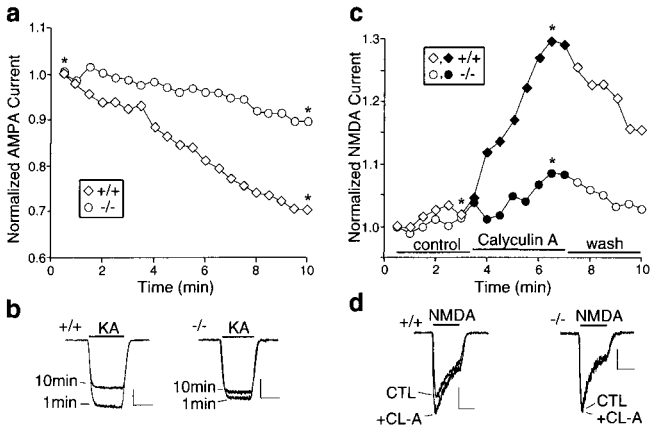

Fig. 4. Dysregulation of glutamate receptor current in spinophilin knockout mice. (*a*) Time course of AMPA receptor current amplitude in acutely dissociated striatal neurons from wild-type and knockout mice. (*b*) Traces for recordings at 1 min and 10 min, as indicated by asterisks in *a*. (Bars = 0.5 nA, 1 sec.) (*c*) Effects of calyculin A (1 μM) on NMDA receptor current in hippocampal neurons from wild-type and knockout mice. (*d*) Traces for recordings, before (CTL) and during (+CL-A) application of calyculin A (1 μM), as indicated by asterisks in *c*. (Bars = 0.2 nA, 1 sec.)

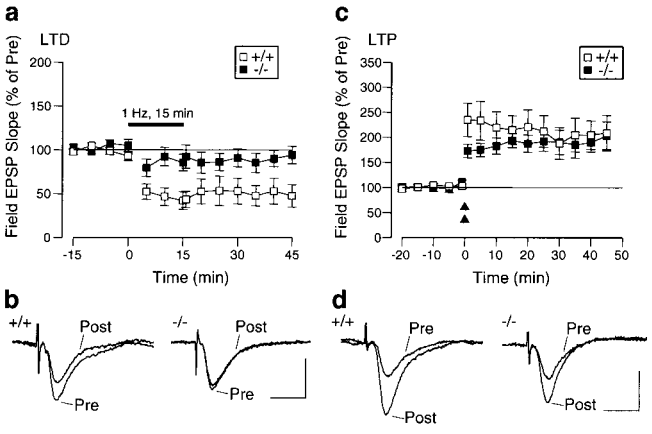

Fig. 5. Reduction of LTD, but not LTP, in spinophilin knockout mice. (*a*) LTD in wild-type and knockout mice after low-frequency stimulation. (*b*) Representative traces for recordings before (Pre) and 45 min after (Post) low-frequency stimulation. (Bars = 1 mV, 10 msec.) (*c*) LTP in wild-type and knockout mice in response to high-frequency stimulation. Double triangles indicate two tetanic stimulations (100 Hz for 1 sec each, with a 20-sec interval). (*d*) Representative traces for recordings before (Pre) and 45 min after (Post) high-frequency tetanic stimulation. (Bars = 1 mV, 10 msec.)

Because PP-1 also plays a role in the regulation of NMDA receptors (28, 38, 39), we examined the involvement of spinophilin in the modulation of NMDA receptor currents. Inhibiting PP-1/2A with calyculin A reversibly enhanced NMDA receptor currents in acutely dissociated hippocampal neurons from wild-type mice (24.8 $\pm$ 5.6% increase, $n = 6$). However, this effect was attenuated significantly in the spinophilin knockouts (4.5 $\pm$ 1.9% increase, $n = 7$, $P < 0.05$ vs. wild-type). A representative experiment is shown in Fig. 4 *c* and *d*. These results indicate that PP-1 cannot effectively regulate NMDA receptors in the absence of spinophilin, suggesting that spinophilin may also target PP-1 to NMDA receptors. In contrast, the dopamine D_1 agonist-induced, PP-1-mediated increase of γ-aminobutyric acid type A ($GABA_A$) receptor currents (40) was similar in wild-type and spinophilin knockout mice (data not shown). The coenrichment of glutamate receptors and spinophilin in dendritic spines, together with the results on AMPA, NMDA, and $GABA_A$ receptors, suggest that spinophilin may specifically modulate excitatory neurotransmission through anchoring PP-1 in the proximity of ionotropic glutamate receptors.

Spinophilin Knockout Mice Exhibit Reduced LTD, but Normal LTP. Because the above studies indicated that spinophilin regulates glutamate receptors, we examined the possible role of spinophilin in two major forms of synaptic plasticity in the Schaffer collateral/CA1 pathway in hippocampal slices: LTD and LTP. LTD induced by low-frequency stimulation (1 Hz, 15 min) was 49.6 $\pm$ 13.6% of prestimulation value in the wild-type mice ($n = 6$) and was greatly reduced in the knockout mice (93.1 $\pm$ 9.4% of prestimulation value, $n = 8$; $P < 0.01$) (Fig. 5 *a* and *b*). In contrast, there was no significant change in LTP induced by a two-train tetanic stimulation (wild type: 207.0 $\pm$ 40.4% of prestimulation value, $n = 8$; knockout: 193.9 $\pm$ 22.3% of prestimulation value, $n = 8$; $P > 0.3$; Fig. 5 *c* and *d*). Paired-pulse facilitation, a form of presynaptic plasticity, also was unaffected (data not shown). These results complement previous studies showing that PP-1 is required for LTD (41, 42). Thus, it is likely that spinophilin localizes PP-1 activity to those substrates in spines that mediate the induction of LTD. In contrast, the lack of change in LTP is consistent with the observation that PP-1 activity is not required for its induction (41, 43).

Spinophilin Knockout Mice Are Resistant to Kainate-Induced Seizures and Neuronal Apoptosis. The altered regulation of glutamate receptors in spinophilin knockout mice led us to examine the possible involvement of spinophilin in kainate-induced seizures. Intraperitoneal injection of kainate at 20 mg/kg caused multiple episodes of severe systemic seizures in wild-type mice, but either no seizure or very mild partial seizures in knockout littermates (Fig. 6*a*). The resistance to kainate-induced seizures was no longer observed when the dosage was increased to the sublethal level of 30 mg/kg (Fig. 6*a*). To test seizure resistance of spinophilin knockout mice to a convulsant not acting directly on the glutamatergic system, we also measured seizures caused by PTZ, which targets the GABAergic system. Spinophilin knockout mice were partially resistant to PTZ-induced seizures at 60 mg/kg dosage, but not at the sublethal dosage of 90 mg/kg (Fig. 6*b*).

Systemic administration of kainate causes apoptosis in hippocampal neurons (33, 44, 45). However, in the spinophilin knockout mice, kainate (20 mg/kg) failed to induce apoptosis in CA1 neurons. Seven days after kainate injection, wild-type neurons exhibited cell death with shrunken cell bodies (Fig. 6*c*). In contrast, the spinophilin$^{-/-}$ neurons showed a normal morphology (Fig. 6*d*), which was similar to that of saline-injected wild-type and knockout mice (data not shown). When TUNEL staining was performed on these neurons, the wild-type tissue showed a strong, positive signal for broken DNA ends, a hallmark for apoptosis, whereas the tissue from spinophilin knockout mice had virtually no apoptotic neurons (Fig. 6 *e–h*). In other experiments, high-density hippocampal cultures were treated with 100 μM glutamate for 24 h and then analyzed by TUNEL staining for excitotoxicity-induced apoptosis. In the wild-type cultures, 39.2 $\pm$ 3.1% of the neurons died by apoptosis; in contrast, only 10.0 $\pm$ 1.3% of spinophilin$^{-/-}$ neurons died ($n = 5$, $P < 0.001$), confirming the protective effects of the spinophilin null mutation. It seems likely that the alteration in the physiological properties of glutamate receptors in the spinophilin$^{-/-}$ mice contributes to the loss of susceptibility to seizures and apoptosis of these mice.

Discussion

The results of the present study provide molecular and cellular evidence that spinophilin plays an important role in the forma-

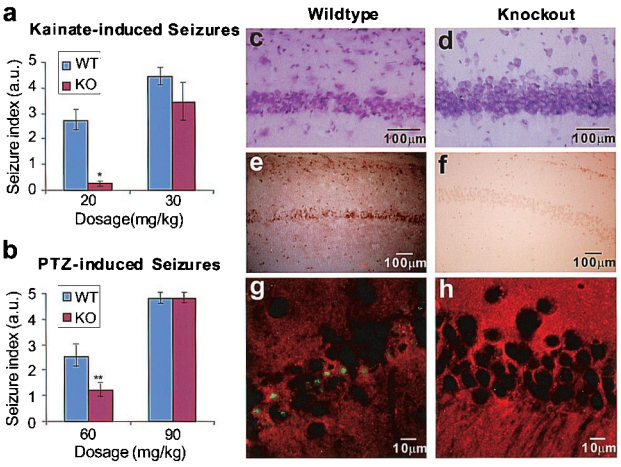

Fig. 6. Effects of spinophilin null mutation on kainate- and PTZ-induced seizures and apoptosis. (*a*) Kainate-induced seizures in wild-type (WT) and knockout (KO) mice. *, $P < 0.001$, compared with WT ($n = 14$ for WT; $n = 13$ for KO). (*b*) PTZ-induced seizures in WT and KO mice. **, $P < 0.05$, compared with WT ($n = 12$ for WT and KO). (*c* and *d*) Cresyl violet staining of hippocampal CA1 neurons from wild-type (*c*) and knockout (*d*) mice 1 week after systemic injection of kainate. Shrinkage because of cell death, seen in wild-type neurons, was not present in neurons from the knockout mice. (Bars = 100 μm.) (*e*—*h*) TUNEL staining. (*e* and *f*) Light microscopy of hippocampal CA1 neurons from wild-type (*e*) and knockout (*f*) mice. Positive staining in the wild type demonstrated that neuronal death was due to apoptosis. (Bars = 100 μm.) (*g* and *h*) Confocal microscopy of cell bodies of CA1 neurons from wild-type (*g*) and knockout (*h*) mice. Broken DNA ends were labeled with FITC (green). The slices then were counterstained with an irrelevant rhodamine-conjugated secondary antibody (red) to highlight the tissue. (Bars = 10 μm.)

tion and function of dendritic spines. Spinophilin-deficient mice displayed an increased number of spines early in development. Moreover, cultured neurons from the knockout mice had more filopodia or spine-like protrusions but the same number of nerve terminals compared with that from wild-type mice. The exact manner by which spinophilin regulates filopodial dynamics and whether this involves an effect on filopodial extension or retraction await quantitative analyses of the growth rate of these protrusions at various developmental stages using live imaging and three-dimensional reconstruction by electron microscopy.

There are several possible mechanisms by which spinophilin might regulate the dynamic morphological changes of filopodia. One such mechanism would be an interaction with the actin cytoskeleton (22), because altering the state of polymerization of actin is known to affect spine morphology (18). Spinophilin has an actin-binding domain at its N terminus and can bundle F-actin filaments (22). Within the actin-binding domain of spinophilin, there are several consensus phosphorylation sites for protein kinase A (PKA), protein kinase C (PKC), and Ca^{2+}/calmodulin-dependent kinases. Phosphorylation of spinophilin by one or more of these kinases might regulate the interaction between spinophilin and actin, thereby reorganizing the actin-based cytoskeleton in dendritic spines.

Another possible mechanism by which spine formation might be altered in the knockout mice is through PP-1-mediated changes in the phosphorylation state of the actin cytoskeleton. It has been shown that PP-1 regulates cell morphology by dephosphorylation of the actin cytoskeleton (46). Spinophilin, through its PP-1-binding domain, is thought to recruit PP-1 to dendritic spines, thus facilitating the dephosphorylation of targeted substrates. The direct interactions of spinophilin with actin and PP-1 may provide a highly localized mechanism for regulating the phosphorylation state of the actin cytoskeleton.

Regulation of glutamate receptor activity by spinophilin provides another possible mechanism for the effect on spine density. Previous studies indicated that AMPA receptor activity is required for the maintenance of dendritic spines. Application of AMPA receptor agonists to hippocampal slice cultures can specifically restore the loss of dendritic spines caused by lesions (14). In the spinophilin knockout mice, AMPA receptor currents were more persistent, presumably because of the removal of PP-1 from the immediate vicinity of AMPA receptors. This is functionally equivalent to increased application of AMPA, which is capable of producing more dendritic spines under lesion conditions. It is conceivable that increased AMPA receptor currents in the spinophilin knockout mice may lead to biochemical changes in the filopodia to enhance their structural stability.

The present study is consistent with a role for spinophilin as a targeting protein for PP-1. The substrate specificity of the pleiotropic enzyme PP-1 is thought to be achieved by a multitude of binding partners (47–49). A variety of cellular processes are dependent on the precise localization of the catalytic subunit of PP-1. Spinophilin, by targeting PP-1 to specific substrates in dendritic spines, controls the phosphorylation states of these substrates. Among them, the AMPA and NMDA receptors play critical functions in synaptic transmission and plasticity. Previous studies suggested that PP-1 regulates the activity of these channels (27, 28). Our present data have provided physiological evidence that spinophilin plays an important role in regulating glutamate receptors by anchoring PP-1 in the proximity of AMPA and NMDA receptors. In the absence of spinophilin, AMPA receptors were no longer subjected to down-regulation by PP-1, which resulted in more persistent AMPA receptor currents. The enhancement of NMDA receptor currents by PP-1 inhibitors seen in the wild-type mice was greatly attenuated in the knockout mice, suggesting that modulation of NMDA receptors by PP-1 also was lost in spinophilin-deficient neurons. Although there are other PP-1-binding proteins in dendritic spines, the functional uncoupling of PP-1 from AMPA and NMDA receptors in the spinophilin knockout mice indicates that spinophilin plays a key role in the regulation of their activities.

Dysregulation of glutamate receptor currents in spinophilin-deficient neurons apparently leads to specific changes in neuronal circuits. Thus, long-term depression was greatly reduced in the knockout mice, whereas long-term potentiation and paired-pulse facilitation were unchanged. These observations are consistent with previous studies on the critical involvement of PP-1 in LTD, but not in LTP (41–43). Our results demonstrate that spinophilin is crucial for certain forms of synaptic plasticity, such as LTD, but not LTP.

The possible contribution of the alteration of AMPA receptor currents to the effects on kainate-induced seizures and apoptosis, seen in the spinophilin knockout mice, will require further studies. In addition, it is possible that the effects of spinophilin deletion on seizures and apoptosis might be attributable to the regulation by PP-1 of targets other than glutamate receptors.

Another intriguing phenotype of spinophilin knockout mice is the reduction in brain size, especially that in the hippocampus. This decrease could be due to a reduction in cell number, length, or size of the dendritic tree, single-cell volume, or extracellular space. The exact cause for the reduction awaits thorough morphological measurements. One possible mechanism underlying this phenotype might be the interaction between spinophilin and $p70^{S6k}$. As documented for neurabin (50), spinophilin interacted with $p70^{S6k}$ *in vitro* (P.B.A. and P.G., unpublished observation). $P70^{S6k}$ is critically involved in the regulation of protein synthesis and cell growth (35, 36). It is possible that spinophilin may influence localized protein synthesis through its interaction with $p70^{S6k}$ and thus might contribute to the observed reduction in brain size and body weight.

In conclusion, our results indicate that spinophilin is involved in the regulation of spine density and synaptic activity; it may be an important component of the intracellular mechanisms linking those two parameters.

We thank George J. Augustine (Duke University Medical Center), Vincent A. Pieribone (Yale University Medical School), and Timothy A. Ryan (Cornell University Medical College) for discussion and comments on the manuscript. We thank Cassandra M. Kirk and Rose J. Payyapilli for excellent technical assistance and The Rockefeller University Transgenic Animal Service for blastocyst injections. This work was supported by National Institutes of Health Grants MH40899 and DA10044 (P.G.), Theodore and Vada Stanley Foundation Research Award (P.G. and J.F.), National Alliance for Research on Schizophrenia and Depression Young Investigator Award (Z.Y.), Northwestern Institute for Neuroscience (A.F.), and the National Institute on Drug Abuse and National Institute of Neurological Disorders and Stroke (M.Z.).

1. Harris, K. M. & Kater, S. B. (1994) *Annu. Rev. Neurosci.* **17,** 341–371.
2. Moser, M. B., Trommald, M. & Andersen, P. (1994) *Proc. Natl. Acad. Sci. USA* **91,** 12673–12675.
3. Horn, G., Bradley, P. & McCabe, B. J. (1985) *J. Neurosci.* **5,** 3161–3168.
4. Lisman, J. E. & Harris, K. M. (1993) *Trends Neurosci.* **16,** 141–147.
5. Calverley, R. K. & Jones, D. G. (1990) *Brain Res. Rev.* **15,** 215–249.
6. Edwards, F. A. (1995) *Physiol. Rev.* **75,** 759–787.
7. Harris, K. M., Jensen, F. E. & Tsao, B. (1992) *J. Neurosci.* **12,** 2685–2705.
8. Boyer, C., Schikorski, T. & Stevens, C. F. (1998) *J. Neurosci.* **18,** 5294–5300.
9. Murphy, D. D. & Segal, M. (1996) *J. Neurosci.* **16,** 4059–4068.
10. Woolley, C. S. & McEwen, B. S. (1992) *J. Neurosci.* **12,** 2549–2554.
11. Harris, K. M. (1999) *Curr. Opin. Neurobiol.* **9,** 343–348.
12. Maletic-Savatic, M., Malinow, R. & Svoboda, K. (1999) *Science* **283,** 1923–1927.
13. Engert, F. & Bonhoeffer, T. (1999) *Nature (London)* **399,** 66–70.
14. McKinney, R. A., Capogna, M., Durr, R., Gahwiler, B. H. & Thompson, S. M. (1999) *Nat. Neurosci.* **2,** 44–49.
15. Svoboda, K., Tank, D. W. & Denk, W. (1996) *Science* **272,** 716–719.
16. Denk, W., Yuste, R., Svoboda, K. & Tank, D. W. (1996) *Curr. Opin. Neurobiol.* **6,** 372–378.
17. Wickens, J. (1988) *Prog. Neurobiol.* **31,** 507–528.
18. Fischer, M., Kaech, S., Knutti, D. & Matus, A. (1998) *Neuron* **20,** 847–854.
19. Yuste, R., Majewska, A., Cash, S. S. & Denk, W. (1999) *J. Neurosci.* **19,** 1976–1987.
20. Carroll, R. C., Lissin, D. V., von Zastrow, M., Nicoll, R. A. & Malenka, R. C. (1999) *Nat. Neurosci.* **2,** 454–460.
21. Shi, S. H., Hayashi, Y., Petralia, R. S., Zaman, S. H., Wenthold, R. J., Svoboda, K. & Malinow, R. (1999) *Science* **284,** 1811–1816.
22. Satoh, A., Nakanishi, H., Obaishi, H., Wada, M., Takahashi, K., Satoh, K., Hirao, K., Nishioka, H., Hata, Y., Mizoguchi, A., *et al.* (1998) *J. Biol. Chem.* **273,** 3470–3475.
23. Allen, P. B., Ouimet, C. C. & Greengard, P. (1997) *Proc. Natl. Acad. Sci. USA* **94,** 9956–9961.
24. Ouimet, C. C., da Cruz e Silva, E. F. & Greengard, P. (1995) *Proc. Natl. Acad. Sci. USA* **92,** 3396–3400.
25. Greengard, P., Allen, P. B. & Nairn, A. C. (1999) *Neuron* **23,** 435–447.
26. Yan, Z., Hsieh-Wilson, L., Feng, J., Tomizawa, K., Allen, P. B., Fienberg, A. A., Nairn, A. C. & Greengard, P. (1999) *Nat. Neurosci.* **2,** 13–17.
27. Wang, L. Y., Salter, M. W. & MacDonald, J. F. (1991) *Science* **253,** 1132–1135.
28. Wang, L. Y., Orser, B. A., Brautigan, D. L. & MacDonald, J. F. (1994) *Nature (London)* **369,** 230–232.
29. Coggeshall, R. E. (1992) *Trends Neurosci.* **15,** 9–13.
30. Izzo, P. N., Graybiel, A. M. & Bolam, J. P. (1987) *Neuroscience* **20,** 577–587.
31. Ferreira, A., Han, H. Q., Greengard, P. & Kosik, K. S. (1995) *Proc. Natl. Acad. Sci. USA* **92,** 9225–9229.
32. Zhuo, M., Hu, Y., Schultz, C., Kandel, E. R. & Hawkins, R. D. (1994) *Nature (London)* **368,** 635–639.
33. Mulle, C., Sailer, A., Perez-Otano, I., Dickinson-Anson, H., Castillo, P. E., Bureau, I., Maron, C., Gage, F. H., Mann, J. R., Bettler, B., *et al.* (1998) *Nature (London)* **392,** 601–605.
34. Nakanishi, H., Obaishi, H., Satoh, A., Wada, M., Mandai, K., Satoh, K., Nishioka, H., Matsuura, Y., Mizoguchi, A. & Takai, Y. (1997) *J. Cell Biol.* **139,** 951–961.
35. Shima, H., Pende, M., Chen, Y., Fumagalli, S., Thomas, G. & Kozma, S. C. (1998) *EMBO J.* **17,** 6649–6659.
36. Montagne, J., Stewart, M. J., Stocker, H., Hafen, E., Kozma, S. C. & Thomas, G. (1999) *Science* **285,** 2126–2129.
37. Ziv, N. E. & Smith, S. J. (1996) *Neuron* **17,** 91–102.
38. Westphal, R. S., Tavalin, S. J., Lin, J. W., Alto, N. M., Fraser, I. D., Langeberg, L. K., Sheng, M. & Scott, J. D. (1999) *Science* **285,** 93–96.
39. Snyder, G. L., Fienberg, A. A., Huganir, R. L. & Greengard, P. (1998) *J. Neurosci.* **18,** 10297–10303.
40. Yan, Z. & Surmeier, D. J. (1997) *Neuron* **19,** 1115–1126.
41. Mulkey, R. M., Herron, C. E. & Malenka, R. C. (1993) *Science* **261,** 1051–1055.
42. Mulkey, R. M., Endo, S., Shenolikar, S. & Malenka, R. C. (1994) *Nature (London)* **369,** 486–488.
43. Blitzer, R. D., Connor, J. H., Brown, G. P., Wong, T., Shenolikar, S., Iyengar, R. & Landau, E. M. (1998) *Science* **280,** 1940–1942.
44. Yang, D. D., Kuan, C. Y., Whitmarsh, A. J., Rincon, M., Zheng, T. S., Davis, R. J., Rakic, P. & Flavell, R. A. (1997) *Nature (London)* **389,** 865–870.
45. Nadler, J. V., Perry, B. W. & Cotman, C. W. (1978) *Nature (London)* **271,** 676–677.
46. Fernandez, A., Brautigan, D. L., Mumby, M. & Lamb, N. J. (1990) *J. Cell Biol.* **111,** 103–112.
47. Hubbard, M. J. & Cohen, P. (1993) *Trends Biochem. Sci.* **18,** 172–177.
48. Cohen, P. (1990) *Adv. Second Messenger Phosphoprotein Res.* **24,** 230–235.
49. Faux, M. C. & Scott, J. D. (1996) *Trends Biochem. Sci.* **21,** 312–315.
50. Burnett, P. E., Blackshaw, S., Lai, M. M., Qureshi, I. A., Burnett, A. F., Sabatini, D. M. & Snyder, S. H. (1998) *Proc. Natl. Acad. Sci. USA* **95,** 8351–8356.